Experimental Modal Analysis of Distinguishing Microstructural Variations in Carbon Steel SA516 by Applied Heat Treatments, Natural Frequencies, and Damping Coefficients

Mohammadreza Ahmadpar[1], Siamak Hoseinzadeh[2,*], Fardis Nakhaei[3] & Saim Memon[4]

1. Department of Mechanical Engineering, Shahid Beheshti University, Tehran, Iran
2. Department of Mechanical and Aeronautical Engineering, University of Pretoria, Pretoria, 002, South Africa
3. Iran Mineral Processing Research Centre (IMPRC), Tehran, Iran
4. Solar Thermal Vacuum Engineering Research Group, School of Engineering, London Centre for Energy Engineering, London South Bank University, London, SE1 0AA, UK

*Correspondence to Siamak Hoseinzadeh. Emails: Hoseinzadeh.siamak@gmail.com and siamak.hosseinzadeh@uniroma1.it

Abstract

The life assessment of materials that structurally shifts, creating mechanical corrosion and damage, during the operation at high temperatures is one of the most critical areas in the gas turbine power plants. This study investigates the widely used carbon steel grade 55 SA516 in the gas turbine blades at metallographic microscopic level and relating it to natural frequency and damping coefficients. In which heat treatments (aging tests) were applied and compared between multiple samples. The results show pearlite is broken up and converted into the ferrite and spherical carbides at grain boundaries. With an increase in microstructural variations in samples due to heat treatments, the first mode of natural frequency slightly decreases but damping ratio increases significantly. In addition, the experimental results show that by increasing the heat treatment time, the Young's modulus decreases by 10.74% and the natural frequency of the second to sixth states of carbon steel also decreases between 4.14 and 4.59%, respectively. As such, the damping coefficients of the second to sixth states increased between 5,609 and 6391 times than their original values, and no connection was obtained between the vibration number and the damping coefficient.

Keywords: aging heat treatment, carbon steel, damping, microstructure change, natural frequency

Introduction

The life assessment of materials that structurally shifts, creating mechanical corrosion and damage, during the operation at high temperatures is one of the most critical areas in the power plant industry. Mechanical corrosion and damage to industrial materials, such as carbon steel, are initiated at microstructural level when subjected to the long-term overheating operation that eventually decreases the life time of the materials. To assess the microstructural variations and residual life of heated materials utilized in the steam/gas/nuclear power plants, destructive and non-destructive tests are used. These tests are costly and complex, it is critical to find an easy and effective way to ensure the quality of heated materials subjected to higher temperatures during industrial load operation. For example, gas turbine blades and boiler pipes are subjected to creep and structural variations during long-term over-heating conditions (Ref 1). Long-term overheating refers to the location of materials at temperatures that cause structural variations over time. A qualitative method for estimating life expectancy was first proposed in Dobrzański et al (Ref 2). In which, samples of steel grade 12 (1Cr-0.5Mo) pipes in operation were tested for estimating life expectancy and the results showed a correlation between rupture strength and microstructural categories based on the degree of spherical carbide (Ref 2). Exploitation at high temperatures leads to various microstructural variations such as variation in the chemical composition of ferrite, structure, size and distance between carbides, solid solution strength and network parameter in alloy steel. Such variations were investigated by Kushima et al. (Ref 3) that utilized 1Cr – 0.5Mo alloy steel for creep at higher temperatures and stresses. The results showed important parameter of the interstitial distance between the carbides. The most obvious point of this model is to link the distance between the carbide particles and the creep life. Adaud et al. (Ref 4) examined the mechanical properties of lithium-aluminum and aluminum-copper-lithium by changing the time and temperature of aging. The results showed, Young's modulus increases and then decreases by about 5%, while shear modulus and Poisson's coefficient remain unchanged.

Ito et al. (Ref 5) examined the effect of aging on damping and modulus of TiNi alloys. In this, aging tests were carried out at 573 K for 30 minutes and then at 673 K for 128 hours. Under these conditions, the Young's modulus decreases and the specific damping coefficient increases sharply. Kariman et al. (2019a) (Ref 6) and Kariman et al (2019b) (Ref 7) simulated freshwater production system utilizes materials subjected to dynamic temperatures consists of heat exchangers, evaporators and condensers that operated with a vacuum pump (Ref 6, 7), and the operating conditions of the system under vacuum pump were examined. Also, the economic analysis of this system and the study of economic parameters on this system in different cities were discussed (Ref 8,9,10). Lunt Jagmer (Ref 11) examined the effect of microstructures on internal friction and the Young's modulus of aged Cu–Be alloy. It showed internal friction and stress decreased after 2 hours of aging at 315°C, and the Young's modulus in long-term aging increased by about 2 GPa compared to short-term aging. Tanaka (Ref 12) examined the effect of grain size and microstructure on internal energy and Young's modulus of a high-strength steel HT-80. It shows the internal energy of ferrite-perlite structures is much higher than that of ferrite-cementite structures of large grain size (Ref 12). Structural variations occur during long-term use of steels at temperatures below the eutectoid temperature that causes the decomposition of perlite into ferrite and spherical carbides and diminution of the strength and hardness of the steel alloys (Ref 13). Microstructural variations are changes that cause major damage during long-term heating operations on metals, which eventually reduces the service life of the materials used in the industrial plant.

In this study, the effect of microstructural changes on the natural frequency and damping at different heat treatment time periods of the carbon steel samples are investigated. This method can be developed in the future for certain components and other materials. To achieve this goal, carbon steel samples "SA516-Grade55" have been prepared and studied. The modal method was used to analyze the system, and the results are compared experimentally and validated with the research literature.

Experimental Research Methodology

Modal Analysis Approach

Modal analysis is the process of determining the inherent dynamic properties of a system in the form of natural frequencies, damping coefficients, mode shapes, and applying them to create a mathematical model of the system's dynamic behavior (Ref 14). The mathematical model is called the modal system model and the information about its properties is called modal data. A typical modal analysis is based on the fact that the vibration response of a time-constant linear dynamic system can be represented as a linear combination of a simple harmonic motion set called natural vibrational modes. Modal analysis is needed to better understand the dynamic behavior of structures and to optimize their dynamic properties. Modal analysis has now entered many engineering and scientific fields. Its applications have expanded from automotive and aerospace engineering to biomechanics, medicine and basic sciences, so that numerical and experimental modal analyses have become two fundamental pillars in structural dynamics (Ref 15).

In this research, the dimensions of the specimens are rectangular in shape and the ratio of length to height of the beam is high, and the displacement due to the transverse shear force versus bending is neglected. This type of beam is called Euler-Bernoulli Can. The first natural frequency of the two free ends of the beam can be written as shown in Eq 1 (Ref 14).

$$f_1 = \frac{1}{2\pi}\left[\frac{22.373}{l^2}\right]\sqrt{\frac{EI}{\rho A}} \qquad (1)$$

The modal analysis in the frequency domain is based on the fit of the curve on the test data with the help of a predetermined mathematical model on the structure. This model includes information on the number of degrees of structural freedom, the damping model, and possibly the number of vibration modes in the measured frequency range. Model hypotheses dictate the mathematical expressions of the curvature of each frequency response. As a result, the main task in this section is to fit the curve in order to extract the modal parameters using experimental data.

The picking method is the simplest one degree of freedom in modal analysis. This method is also called halve-power. This method is directly based on the assumption of a degree of freedom. In this method, data in the resonance range, such as the data of a single-degree system, are treated (Ref 16). The steps are as follows:

The natural frequency of the selected mode is obtained by the frequency response function peak.

$$|\alpha_r(w)|_{\max} \rightarrow \ \mathrm{W}_r = W_{peak} \qquad (2)$$

Damping is a property of the material by which mechanical energy is wasted in a vibrating system, which is usually a conversion of mechanical energy into heat energy. The damping test is performed using the free-free beam vibration frequency response method at room temperature, which measures the material's damping properties quickly and easily. The measurement is such that the sample is first stimulated by the hammer, then the amplitude of the vibration gradually decreases with time. The vibrational frequency and amplitude reduction are transmitted to the computer by the accelerometer. The reduction in the amplitude is a function of the vibration time and mode as detected by pulse-processing software (Ref 11).

Figure 1 shows the maximum amplitude $|\alpha(w_r)|$ which corresponds to the first natural frequency (vibrational mode) of the system, then the frequencies (w_a,w_b) are selected on both sides of the resonant peak with amplitude $\frac{|\alpha_{max},\alpha(w_r)|}{\sqrt{2}}$ (Ref 11).

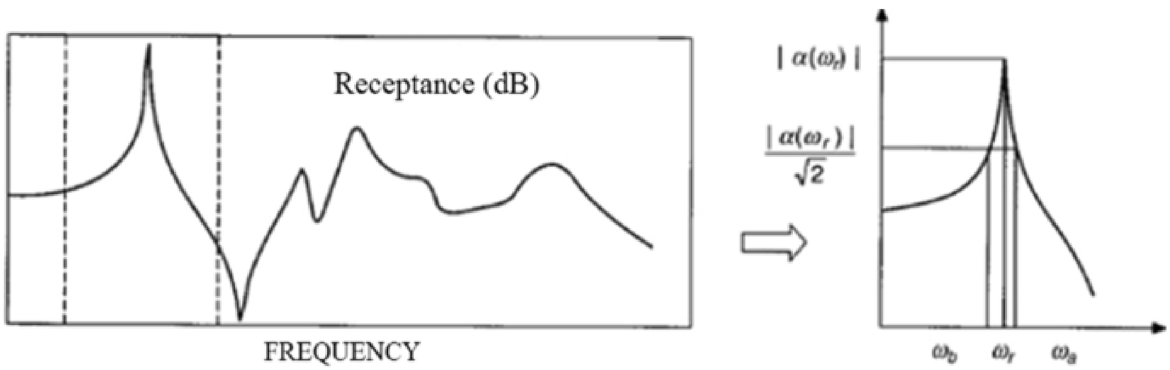

Fig. 1. Diagram of maximum of frequency response function

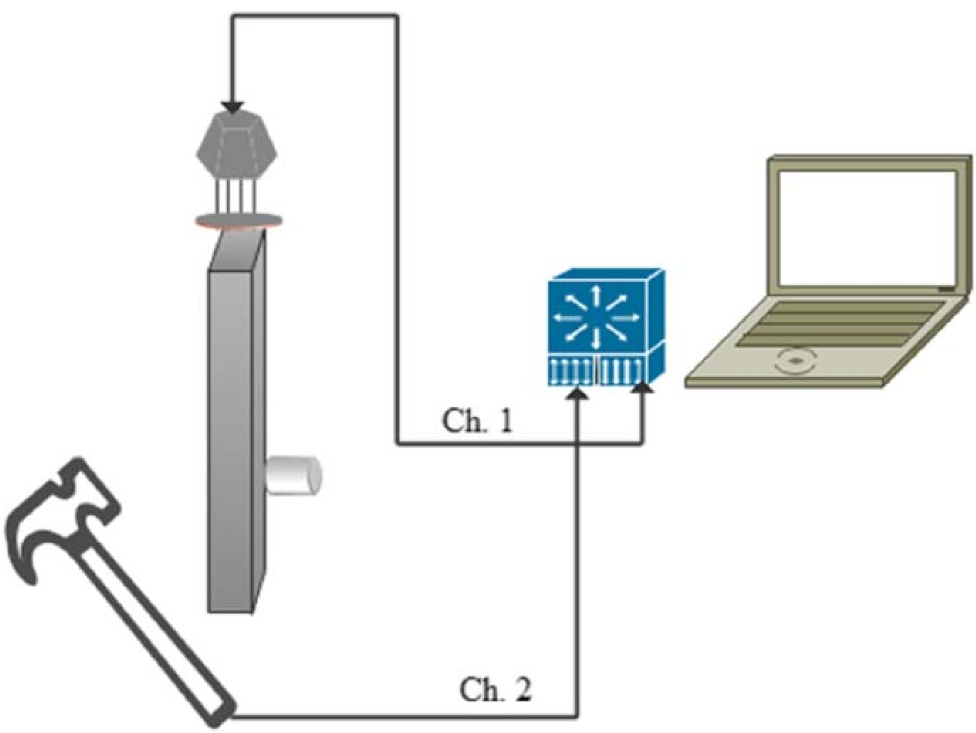

Fig. 2. The general schematic of hammer test with main required equipment

The damping loss factor is obtained with respect to the resonant peak width according to Eq 3 (Ref 17).

$$\eta_r = \frac{W_b^2 - W_a^2}{2W_r^2} \tag{3}$$

where, w_r is the maximum frequency of the graph domain, and w_a,w_b are the resonances on both sides of the resonant peak. The structural damping ratio is shown in Eq 4.

$$\xi = \frac{\eta_r}{2} \tag{4}$$

For small dampings ($\xi \ll 1$) the logarithmic reduction parameter, δ, is defined (Ref 11). This parameter shows the effect of precipitations on the reduction in properties and is defined as in Eq 5 [17].

$$\varsigma = \pi\, Q^{-1} \tag{5}$$

The internal friction (Q^{-1}) is obtained using bandwidth (Δw) and is in the form of Eq 6 (Ref 17).

$$Q^{-1} = \frac{\Delta W}{W_r} = \frac{W_b - W_a}{2W_r} \tag{6}$$

Materials and Equipment

The material used in this study is SA516-grade 55 steel. This steel is ferrite-pearlite steel (low carbon and alloy steel). The reason for choosing this is that it has a very noticeable structural variations during operation in industrial plants. The chemical composition of the sample by weight percent is given in Table 1, validated during experimental tests. Heat treatment of the components was performed in the electric furnace. The pieces were heat treated at a constant temperature of 680°C between 12 and 24 hours.

Table 1 Chemical composition of steel SA516 Grade55

C	Si	Mn	P	Mo	Cr	Ni
0.15	0.20	0.93	0.012	0.01	0.002	0.02

Experimental modal analysis consists of two stages of preparation for testing: (a) measuring frequency response, (b) extracting modal parameters. In order to prepare the components, a sample was designed with its natural frequencies within the range of the modal analyzer (max. 6000 Hz) and the natural frequency of the first sample was within the natural frequencies of the device due to measurement device limitation. To prepare the components for testing, the appropriate dimensions of the specimens were calculated, as according to the original dimensions of the sheet available for prototyping, i.e., 300mm ×

26mm × 6 mm. To increase the reliability and error reduction, two pieces of heat treatment were prepared for each sample.

By placing the moment of inertia of the cross in terms of width and thickness in Eqs. 1, 7 is obtained.

$$f_1 = \frac{1}{2\pi}[\frac{22.373}{l^2}]\frac{h}{L^2}\sqrt{\frac{E}{\rho}} \tag{7}$$

According to Eq 7, the natural frequency is influenced by the length and thickness of the sample so as the need for the test. Since the thickness of the sheet available for prototyping is about 6 mm and due to heat treatment, the layer on it (up to one millimeter) is removed by oxidation during heat treatment and subsequent surface treatment, so the thickness is approximately 5 mm, using Abacus software trial and error 150 mm length was selected, final dimensions for testing were 147.80mm × 29.30mm × 5.20 mm. With these dimensions, the natural frequency is within the frequency range of the device. Since the sample sizes are very influential in the natural frequency, all samples were measured in micrometers and equal to 0.02 mm. Then all samples were precisely 160/00±0.02 gr.

Figure 2 shows the overview of the modal tester with impact. In which, the frequency response function is calculated after measuring the response time and impulse time signals and applied Fast Fourier transform to it.

Frequency testing is performed in free-standing mode. The procedure is illustrated in Fig 3. The frequency test of each sample is taken several times and the final frequency is the average of several frequencies measured with high coherence.

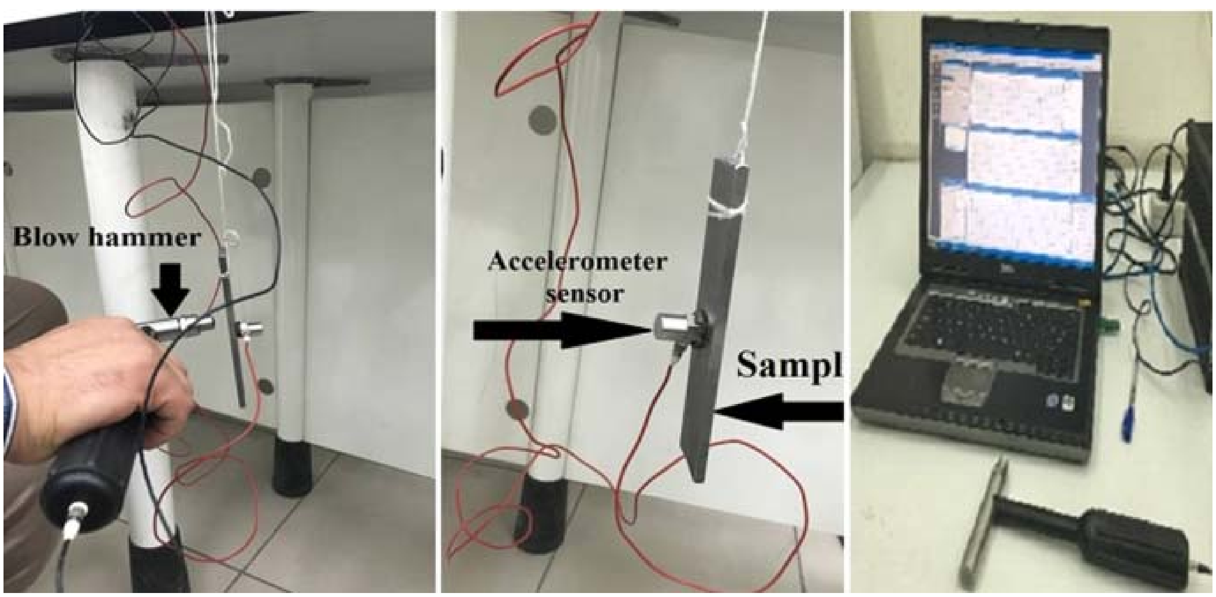

Fig. 3. The frequency test of samples

One of the methods of restructuring in steels is accelerated aging of the sample. For rapid structural changes in the investigated steel, which is carbon steels, heat treatment is performed in the range of 590 to 700 °C. The samples were heat treated at 12 hours and 24 hours periods at 680 °C. At microstructural level, drastic variations in the ferrite-perlite structure were metallographically recorded, in which the perlite areas were clearly decomposed and the structure consisted of ferrite-carbide.

Results and Discussion

The samples were initially metallographically tested to understand the effect of aging heat treatment on the restructuring of carbon steel SA516. First, metallography of the sample before heat treatment is shown in Fig. 4. In which, the light phases are ferrite and the dark phases are perlite. Over time, the perlite phases decompose to ferrous carbide (cementite) and ferrite spheres (Ref 18).

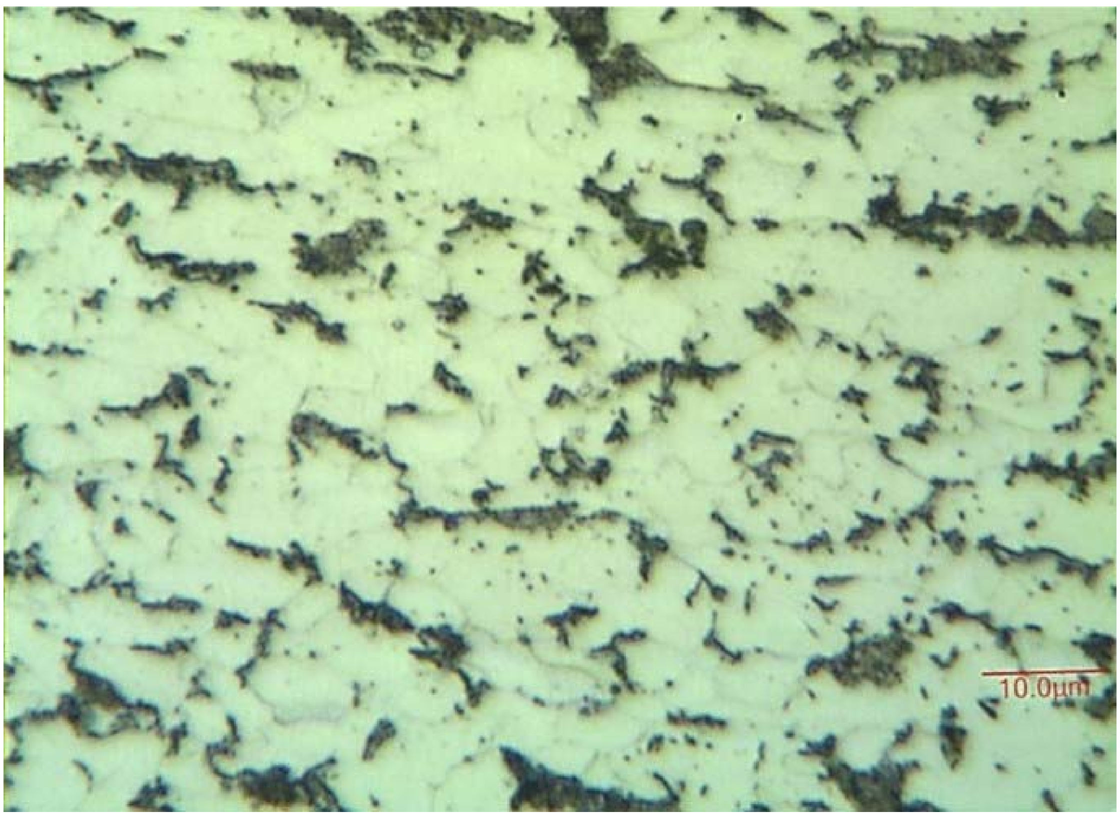

Fig. 4. Metallographic microscopic image of the carbon steel SA516 structure before heat treatment showing the light phases are ferrite and the dark phases are perlite

Figure 5 shows ferrite layers are added to the background phase and the carbides precipitate in the field. Over time, the scattered precipitation layers of cementite join together in the fields and form coarse carbide spheres, as shown in Fig. 6. The presence of carbide in the grain reduces the grain strength. Also, the solubility of the intermediate carbonates of the cementite phase increases in iron and increases the volume of the carbide phase and makes the carbide larger, which was initially mentioned in Kim article (Ref 19) and the laboratory results confirm their validity. Larger particles also grow at the expense of smaller particles. This process, called steward preparation (the absorption of fine particles by larger particles), occurs by penetration to reduce the total joint area between the two phases. On the other hand, the readiness of the steel reduces the strength and hardness of the material. This issue is mentioned in Hertzberg article (Ref 20) and the experimentally results confirm their validity.

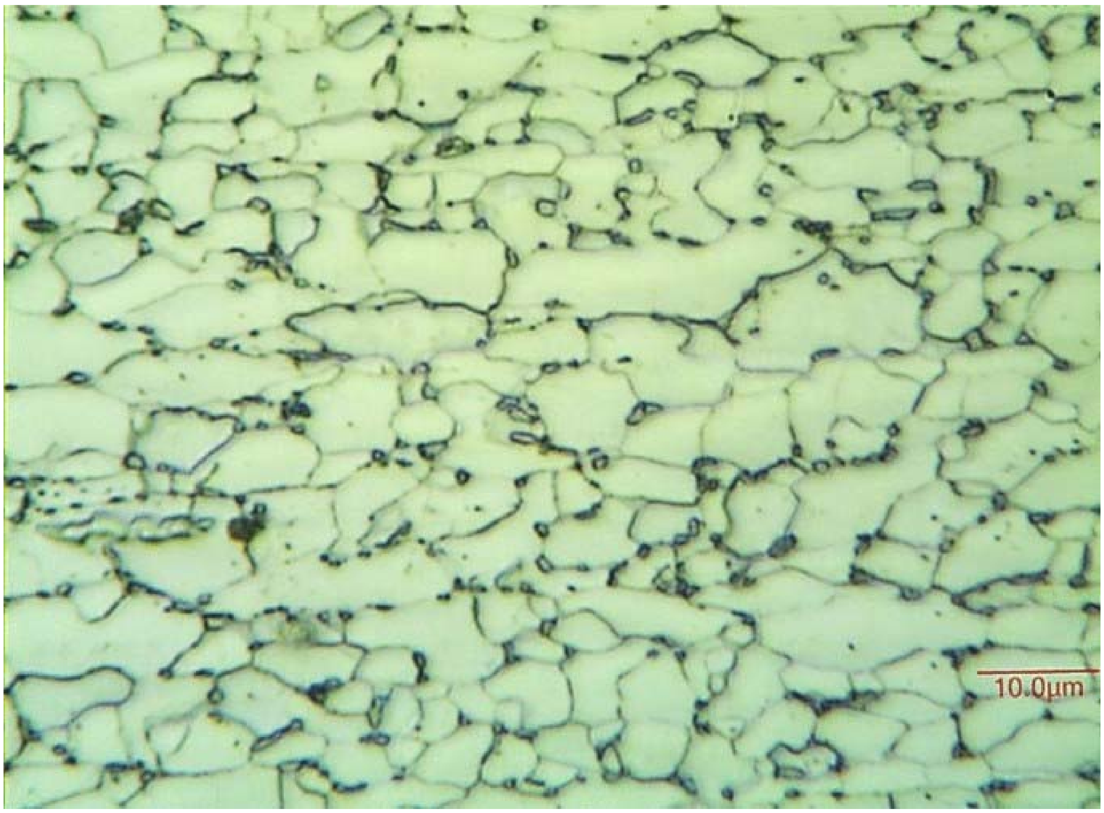

Fig. 5. Metallographic microscopic image of the carbon steel SA516 structure after 12 hours of heat treatment

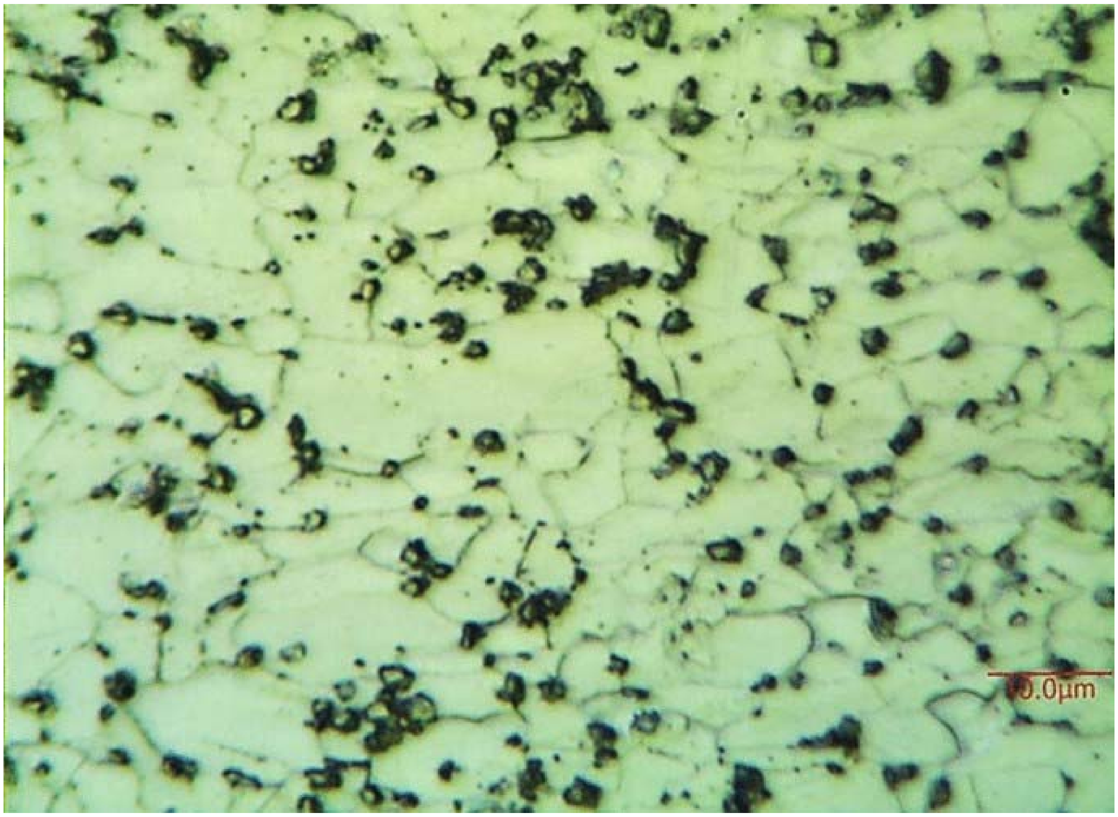

Fig. 6. Metallographic microscopic image of the carbon steel SA516 structure after 24 hours of heat treatment

By performing a tensile test of the specimens (three specimens were fabricated and tested from each piece), it was found that the Young's modulus decreases with an increase in heat treatment time. The results of the tensile test are presented in Table 2.

Table 2 Young's module variations obtained from the tensile test on three specimens

Row	Samples	Young's module GPa	Diff%
1	Not treated sample	190	–
2	Sample after 12 hours heat treatment	187	−4.65
3	Sample after 24 hours heat treatment	182	10.74

Due to a cubical crystal lattice microstructural shape of the carbon steel, such heat treatments also reduced elastic modulus. As the volume of the carbon dioxide-induced network increases, the inter-atomic spring constant decreases followed by the Young's modulus, which is consistent to the observations made in (Ref 19).

The natural frequency of the first mode of the beam was calculated in the free two-state mode using Eq 1. In which, the length, moment of inertia, cross-sectional area, and density of all normal and heat treated samples are equal and differ only in the Young's modulus. As the Young's modulus decreases, the natural frequency of the first mode is expected to decrease, as well as the natural frequency results from the modal test are presented in

Table 3. The results show the natural frequency of the first mode of the sample, decreases with an increase in heat treatment time.

Table 3 The first experimental mode of natural frequency

Row	Samples	natural frequency (Hz)	Diff%
1	not treated sample	1277	–
2	sample after 12 hours heat treatment	1251	−4.65
3	sample after 24 hours heat treatment	1219	−10.74

The damping variations in carbon steel are investigated using the factors of precipitation or intermediate phases with different Young's modulus and high damping as shown in Table 3, these results are consistent with (Ref 21).

Table 4 shows the experimental damping coefficients using Eqs. (2-6). In Table 5, the second to sixth natural frequencies of the samples are presented. In Tables 5 and 6, the damping coefficient and the logarithmic reduction corresponding to these frequencies are presented, respectively.

Table 4 Damping coefficients of samples

Row	Samples	loss factor(η) $*10^{-3}$	Logarithmic Decrement $*10^{-}$	Damping ratio (ξ) * 10^{-3}	Diff with normal sample
1	Not treated sample	6.577	20.665	3.288	–
2	Sample after 12 hours heat treatment	18.437	57.757	9.218	180%
3	Sample after 24 hours heat treatment	38.509	121.124	19.254	450%

Table 5 The 2nd to 6th natural frequency of the samples obtained from the modal analysis

No Freq	Not treated sample	Sample after 12 hours heat treatment (Diff%)	Sample after 24 hours heat treatment (Diff %)
1	3517	3442 (−2.15%)	3356 (−4.59%)
2	3598	3525 (−2.03%)	3439 (−4.42%)
3	6841	6704 (−2.00%)	6558 (−4.14%)
4	7350	7194 (−2.12%)	7013 (−4.59%)
5	11169	10942 (−2.03%)	10674 (−4.43%)

Table 6 Damping coefficients of samples obtained from 2nd to 6th natural frequency ($*10^{-3}$)

No	not treated sample	Sample after 12 hours heat treatment (Diff%)	Sample after 24 hours heat treatment (Diff%)
1	6.231	17.985 (188.6%)	38.019 (510.2%)
2	6.491	18.061 (178.2%)	38.678 (495.9%)
3	6.814	18.512 (171.7%)	38.216 (460.9%)
4	6.027	18.296 (203.6%)	38.519 (539.1%)
5	6.398	18.328 (18.328%)	38.347 (499.4%)

As shown in Tables 4, 5 and 6, the damping ratio has been increased because the surface area of between two to sixth phase with different Young's modulus has increased. This is due to the deposition of carbides in the fields of applied heat for the periods of 12 and 24 hours. As a result of heat treatment, the perlite is broken and the structure of the iron carbide layer is heterogeneously deposited in the surfaces and begins to grow and become spherical with increasing heat treatment time, so that the surfaces become unstable and disappear afterward. The microstructure becomes softer and, as a result, logarithmic reduction and damping ratio increase during the aging process.

Conclusion

In this study, the effects of structural changes on the natural frequency and damping on the samples of SA516-Grade55 carbon steel are investigated aged at 680°C for 12 and 24 hours of heat treatment. The conclusions are summarized as follows:

1- With the metallography of the samples, significant structural changes were observed. As the heat treatment time increased, the perlite decomposed into ferrite and spherical carbides in the surface field.

2- Aging operations in the samples show Young’s modulus decreased by 10.74% at higher heat treatment time.

3- The natural frequency of the first mode of the samples decreased to 4.54% at higher heat treatment time. The natural frequency of the second to sixth modes of carbon steel also decreases between 4.14 and 4.59%. It implicates that the mode number does not have a significant effect on changing the natural frequency of the samples.

4- As the heat treatment time increases, the damping coefficient of the first mode increases to 5,855 times to its original value due to the increase in precipitation of carbides in the grain boundaries, the joint level of the two backgrounds and reinforcing. As the thermal conductivity increases, the attenuation coefficients of the second to sixth modes increased between 5,609 and 6,391 times than their original value, and the relationship between the vibration mode number and the attenuation coefficient cannot be obtained.

References

1. S. Ebrahim T. Moussavi, *Super Heaters*, pp. 45-51,Tehran: Niroo Research Institute, 2008
2. J. Dobrzański A. Hernas, Correlation between Phase Composition and Life-Time of 1Cr-0.5Mo Steels during Long-Term Service at Elevated Temperatures, J. Mater. Proc. Technol., Vol. 53, No. 1-2, pp. 101-108, 1995.-
3. K. Kushima F. Kimura Abe, K. Maruyama, Effect of Microstructural Change on Creep Deformation Behaviour and Long-Term Creep Strength of 1Cr-0.5Mo Steel, J. Iron and Steel Institute of Japan, Vol. 86, pp. 131-137, 2000
4. M.E. O' Dowd, W. Ruch, E.A. Starke, Dependence of Elastic Modulus on Microstruture in 2090-Type Alloys, J. Phys. Colloques, Vol. 48, No. C3, pp. 565-576, 1987
5. K. Ito, T. Moroyama and I. Fukumoto, Effects of Ageing on Damping Capacity of TiNi Alloys, *J. Phys. Colloques*, 1985, **46**(C10), p 645–648.

6. H. Kariman, S. Hoseinzadeh, & P. S. Heyns (2019). Energetic and Exergetic Analysis of Evaporation Desalination System Integrated with Mechanical Vapor Recompression Circulation. Case Studies in Thermal Engineering, 16, 100548
7. H. Kariman, S. Hoseinzadeh, A. Shirkhani, P. S Heyns., & J. Wannenburg (2019). Energy and Economic Analysis of Evaporative Vacuum Easy Desalination System with Brine tank. Journal
8. S. Hoseinzadeh, R. Yargholi, H. Kariman, & P. S Heyns. Exergeoeconomic Analysis and Optimization of Reverse Osmosis Desalination Integrated with Geothermal Energy. Environmental Progress & Sustainable Energy, e13405
9. R. Yargholi, H. Kariman, S. Hoseinzadeh, M. Bidi, & A. Naseri (2020). Modeling and advanced exergy analysis of integrated reverse osmosis desalination with geothermal energy. Water Supply
10. S. Hoseinzadeh, P. S. Heyns, & H. Kariman (2019). Numerical Investigation of Heat Transfer of Laminar and Turbulent Pulsating Al2O3/Water Nanofluid Flow. International Journal of Numerical Methods for Heat & Fluid Flow.
11. L. Yagmur, Effect of Microstructure on Internal Friction and Young's Modulus of Aged Cu–Be Alloy, *Mater. Sci. Eng., A*, 2009, **523**(1–2), p 65–69.
12. M. Tanaka and H. Iizuka, Effects of Grain Size and Microstructures on the Internal Friction and Young's Modulus of a High-Strength Steel HT-80, *J. Mater. Sci.*, 1991, **26**(16), p 4389–4393.
13. J. Dobrzański, H. Krztoń and A. Zieliński, Development of the Precipitation Processes in Low-Alloy Cr-Mo Type Steel for Evolution of the Material State after Exceeding the Assessed Lifetime, *J. Achieve. Mater. Manufac. Eng.*, 2007, **23**(2), p 19–22.
14. S. Singiresu Rao, *Mechanical Vibrations*, pp. 115-123, New York: Prentice Hall, 5th edition, 2011
15. S Singiresu Rao, *Vibration of Continuous Systems*, pp. 245-251 New Jersey: John Wiley & Sons, 2007
16. A. Bertha and J. M. Roesset, Analytical Evaluation of the Accuracy of the Half-power Bandwidth Method to Estimate Damping Ratios in a Structure, *Proceedings of the 4th International Conference on Structural Health Monitoring of Intelligent Infrastructure (SHMII 09),* pp. 2–9, July 2009
17. Maringer, E Robert, *Damping Capacity of materials*, pp. 35-42, Ohio: Battelle Memorial Institute, Columbus Laboratories, 1966
18. R. Visvanatan, *Damage Mechanisms and Life Assessment of High Temperature - Components*, ASM international society, Ohio, 1995, p 112–118
19. S.A. Kim and W.L. Johnson, Elastic Constants and Internal Friction of Martensitic Steel, Ferritic-Pearlitic Steel and α-Iron, *Mater. Sci. Eng., A*, 2007, **452**, p 633–639.
20. Hertzberg, W. Richard, *Deformation and Fracture Mechanics of Engineering Materials*, pp. 108-112, New York: John Wiley & sons, 1989
21. A.-W. El-Morsy, Ahmed IZ Farahat, Effect of Aging Treatment on the Damping Capacity and Mechanical Properties of Mg-6Al-1Zn Alloy, *Sci. World J.*, 2015, **2015**, p 1–8.